Continental Shelf Research 120 (2016) 59–67

Contents lists available at ScienceDirect

Continental Shelf Research

journal homepage: www.elsevier.com/locate/csr

Research papers

Observation of internal tide-induced nutrient upwelling in Hungtsai Trough, a submarine canyon in the northern South China Sea

Su-Cheng Pai*, Ching-Ling Wei, Saulwood Lin, Liang-Saw Wen, Chun-Mao Tseng

Institute of Oceanography, National Taiwan University, Taipei, Taiwan

ARTICLE INFO

Article history:
Received 4 November 2015
Received in revised form
8 March 2016
Accepted 15 March 2016
Available online 15 March 2016

Keywords:
Nutrients
Internal tide
Hungtsai trough
South China Sea, Nutrient flux

ABSTRACT

Temporal variations in hydrographic parameters and nutrients were observed in a 300 m deep submarine canyon (Hungtsai Trough) near the southern tip of Taiwan. A vigorous oscillation below the surface layer has been observed which relates closely to an internal tidal wave generated from the nearby Luzon Strait. The vertical movement can be measured by monitoring an 18 °C isothermal depth which shows an up-and-down oscillation between 90 and 240 m with an average displacement of 110 m within a tidal cycle, a scale significantly larger than has been reported elsewhere. The frequency of this oscillation coincides with the surface tide but in an almost opposite phase. All hydrographic and chemical parameters (oxygen, density, fluorescence, transmittance and nutrients including nitrate, phosphate and silicate) synchronize with the tidal movement, as judged by normalized plots against temperature. When the nutrient-rich deep water upwells and becomes an outcrop over the trough rim at 100 m deep, it is swept horizontally by the strong alongshore tidal current. Consequently, the trough acts as a source point to supply extra nutrients to the coastal ecosystem.

1. Introduction

The southernmost tip of Taiwan is renowned by its large communities of coral reefs in nearshore water along the coastline of the Hengchun Peninsula, which is now a protected area under the administration of Kenting National Park. There is little river run-off in the whole peninsula, therefore one might suspect how coral can obtain enough nutrients to sustain its growth. In the last decade, the question has been revealed to be an upwelling of cold nutrient-rich deep ocean water in Nanwan Bay (Lee et al., 1997; Chen et al., 2004; Chen et al., 2005). Some individual events like typhoon can lead to upwelling (Ko et al., 2009). However, most of the extra nutrient input is induced consistently by an "internal tide" which is generated from the Luzon Strait between Taiwan and the Philippines (Lien et al., 2005; Wong et al., 2007; Jan et al., 2007, 2008; Farmer et al., 2010; Alford et al., 2010, 2011, 2015; Lien et al., 2014). Following the tidal cycle, the deep cold water has a vertical and regular displacement or an up-and-down oscillation. The tidal wave propagates towards the continental shelf and the amplitude can be magnified when it encounters a semi-enclosed basin. Nutrients are dispersed into the surface mixing layer through eddy diffusion (Shea and Broenkow, 1982). Apart from the basin-like topography, the narrow structure of a submarine canyon can also provide such an effect, like Astoria Submarine Canyon off Oregon (Bosley et al.,2004), Perth Submarine Canyon off western Australia (Rennie et al., 2009) and Kaoping Submarine Canyon which is located 100 km north of Hengchun Peninsula (Lee et al., 2009; Chiou et al.,2011). These internal tide related physical processes can bring up extra nutrients to the surface layer, thus enhance local biochemical productions. For example, significant upward nutrient fluxes of up to 22.9 mmol N $m^{-2}hr^{-1}$ and 1.75 mmol P $m^{-2}hr^{-1}$ have been reported in Nanwan Bay (Jan and Chen, 2009).

There is another submarine canyon in southern Taiwan (between Nanwan Bay and Kaoping Canyon) which produces an at least equal nutrient flux, but has received less attention. The canyon is called Hungtsai Trough (Wei et al., 2009, 2012), a U-shaped canyon with a dead end structure which is located just a few kilometers off the west coast of the Hengchun Peninsula facing the South China Sea side. It can be topographically characterized by a 200 m-deep contour line (Fig. 1); which is about 15 km long and 3 km wide in a northwest-southeastly direction, with a central depth of ca. 350 m (Yu and Chiang, 1994). In the early 1970s, the deep trough water was considered as a source of cooling water for the reactor of the nearby Taiwan's Third Nuclear Power Plant. Later, that idea was abandoned due to unstable temperature recorded in the trough (Liang et al., 1985). Now it is known that the unstable temperatures are likely caused by the internal tide. In this study we present our past observations on nutrient oscillation in Hungtsai Trough and explain why the net

* Corresponding author.
E-mail address: scpai@ntu.edu.tw (S.-C. Pai).

http://dx.doi.org/10.1016/j.csr.2016.03.018
0278-4343/

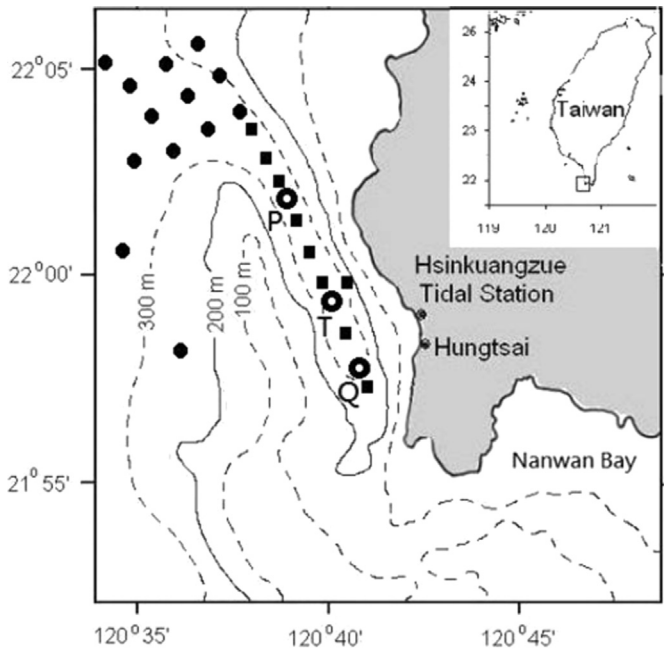

Fig. 1. Location and bottom topography of the Hungtsai Trough. Dots and squares mark 13 out-trough and 9 inner-trough stations during Cruise ORI-194. Circles represent anchored stations P, T and Q. On Cruise 239, repeat observations (back-and-forth between Stations P and Q) were made every other hour over 25 h. On Cruise 419 and 742, profiles at Station T were obtained every hour for 26 and 13 h, respectively.

nutrient flux is much larger here than in other places due to the combined topography-tide effect.

2. Cruise information

Data presented in this work were obtained by the research vessel Ocean Research I (operated by National Taiwan University) during four cruises, namely, ORI-194, 239, 419 and 742 over a 15 year period. On the first cruise, ORI-194 (Jan 17-19, 1989), a total number of 21 stations off the western Hengchun peninsula were investigated. Among them, 12 stations were located outside and the other 9 were inside the Hungtsai Trough (also see Fig. 1). Temperature, salinity and depth data were obtained by a SeaBird SBE-9 CTD attached with oxygen and fluorescence sensors. A year later, the ship revisited the same area (Cruise 239, Jan 4-8, 1990), but this time CTD operations (with oxygen and fluorescence sensors) were carried out at only two stations: Sta. P at the trough entrance and Sta. Q at the far end. The ship moved back-and-forth between these two stations for 25 h at a time interval of ca. 1 h between each two CTD casts. Thus, 13 casts were deployed at Sta. P and 12 casts at Sta. Q.

A more organized survey was arranged during Cruise 419 (May 20-24, 1995), in which onboard wet chemical analysis was included in addition to CTD and attached sensors. Only one anchored location (named Station T, bottom depth 280 m) was chosen for repeat observation over a period of 26 h at a frequency of every hour. Water samples were collected at depths of 3, 20, 40, 60, 80, 100, 125, 150, 175, 200, 225 and 250 m by a rosette sampling system. They were analyzed for concentrations of oxygen, nitrite, nitrate, phosphate and silicate using either manual procedures or a flow injection analyzer onboard the ship within 1 h after sample collection. On a later Cruise 742 (Dec. 24-26, 2004), the same anchored location (Station T) was observed for a period of 13 h using a Seabird SBE-9 CTD system with a fluorescence probe at a frequency of ca. 1 h per cast.

3. Results and discussion

3.1. CTD profiles

Composite profiles of temperature, salinity, sigma-t and oxygen/ fluorescence are plotted separately in Fig. 2 for Cruises 194, 239, 419 and 742. In winter cruises (194 and 239), the surface mixing layer was ca. 100 m thick, but was less significant for Cruise 419 and 742. Large salinity variations were shown for 9 inner casts of Cruise 239, indicating that in the surface layer, horizontal tidal flushing/advection/mixing may all play important role. Below the mixed layer, the water became very dynamic and changed quickly hour by hour. The temperature profiles for all cruises spread out and converged gradually near the bottom. It can also be seen that the scale of oscillation was much more pronounced at the trough end or inside the trough than that at the entrance.

The vertical variation of the water mass can also be presented as time sequence plots, i.e. plot the temperature data at given depths from the surface down to the bottom. In Fig. 3 the plot was made at 10 m intervals for Cruises 194 and 239, and at 5 m for Cruises 419 and 742. All diagrams indicate a general trend of tidal cycles, but if one looks into the fine structures at different depths they indicate that the movements of different water layers are not completely synchronized.

3.2. Center of the oscillation

The variation in the composite temperature profiles serves as an indicator for the center of the oscillation. The maximum temperature variations (ΔT) for the five diagrams shown in Fig. 2 are 4.14, 7.24, 6.37, 6.00 and 7.33 °C at depths of 160, 160, 160, 180 and 175 m, respectively. Even though these results were taken from different cruises, it is reasonable to consider that the center of the vertical oscillation should occur at the depth of maximum variation, i.e. 170 ± 10 m.

3.3. Frequency and amplitude

Since the mean temperature at 170 m is 17.84 °C, the "18 °C contour line" can be used to evaluate the amplitude of the vertical oscillation. Data were sorted for Cruises 239, 419 and 742 and the results are shown in Fig. 4. The surface tide data recorded in the same period at the Hsinkuanzue Tidal Station were also plotted.

On Cruise 239, the 18 °C isothermal line moved between depths of 125 and 225 m at Sta. P during a 10 h period (vertical range 100 m). The upwelling speed can be roughly estimated to be around 10 m hr^{-1}. At Sta. Q the 18 °C line moved from 240 to 130 m within 4 h, giving a vertical speed of 27.5 m hr^{-1}. On Cruise 419 the 18 °C line moved up-and-down twice in a day, with a minimum depth of 110 m and a maximum depth of 220 m. Each up or down movement was completed in 6 h, giving an upward or downward moving speed of ca. 18.3 m hr^{-1}. On Cruise ORI-742, a single semi-diurnal cycle was observed, which showed a minimum depth of 90 m and a maximum of 210 m. The 120 m movement occurred within 6 h, therefore a high upwelling speed of 20 m hr^{-1} was estimated.

In this area, the alongshore current flows in a northwest direction during the flood tide, and in a southeast direction for the ebb tide (Liang et al., 2003). A comparison of the up-and-down movement of the 18 °C line and the surface tidal cycle shows that the frequency is almost the same, but the phase is nearly opposite (although with a 1–2 h lag). During the surface spring tide the 18 °C line sinks to a deeper depth, and *vice versa* (The contour line rises during the surface ebb tide).

It should be noted that the internal tide generated in Luzon Strait may have different moving direction from that of the surface

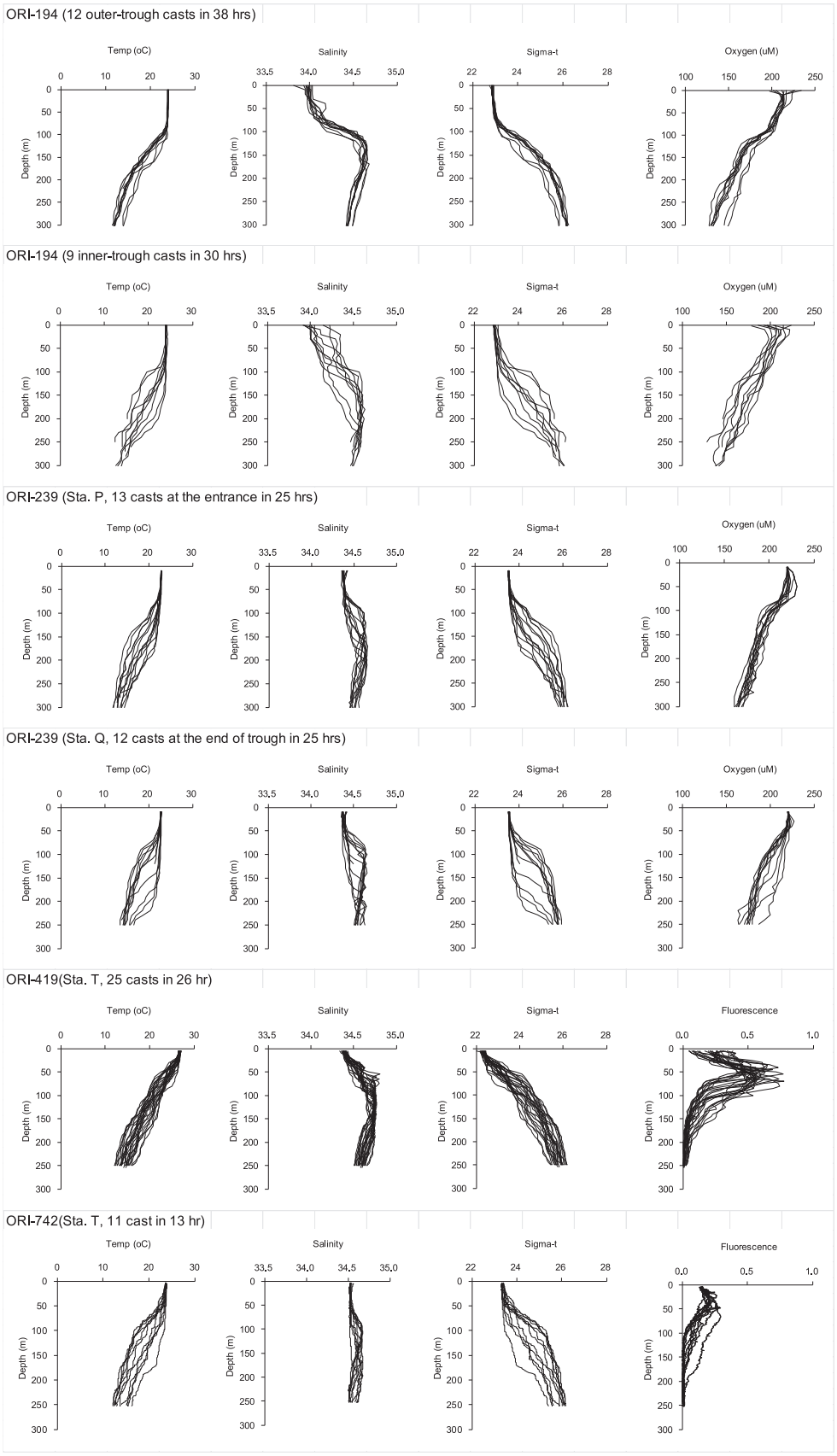

Fig. 2. Composite profiles of temperature, salinity, sigma-t and oxygen/flourescence of (the 1st row) 13 outer-trough casts on Cruise 194, (the 2nd row) 9 inner-trough casts on Cruise 194, (the 3rd row) 13 casts at Station P on Cruise 239, (the 4th row) 12 casts at Station Q on Cruise 239, (the 5th row) 25 casts at Station T on Cruise 419, and (the 6th row) 11 casts at Station T on Cruise 742.

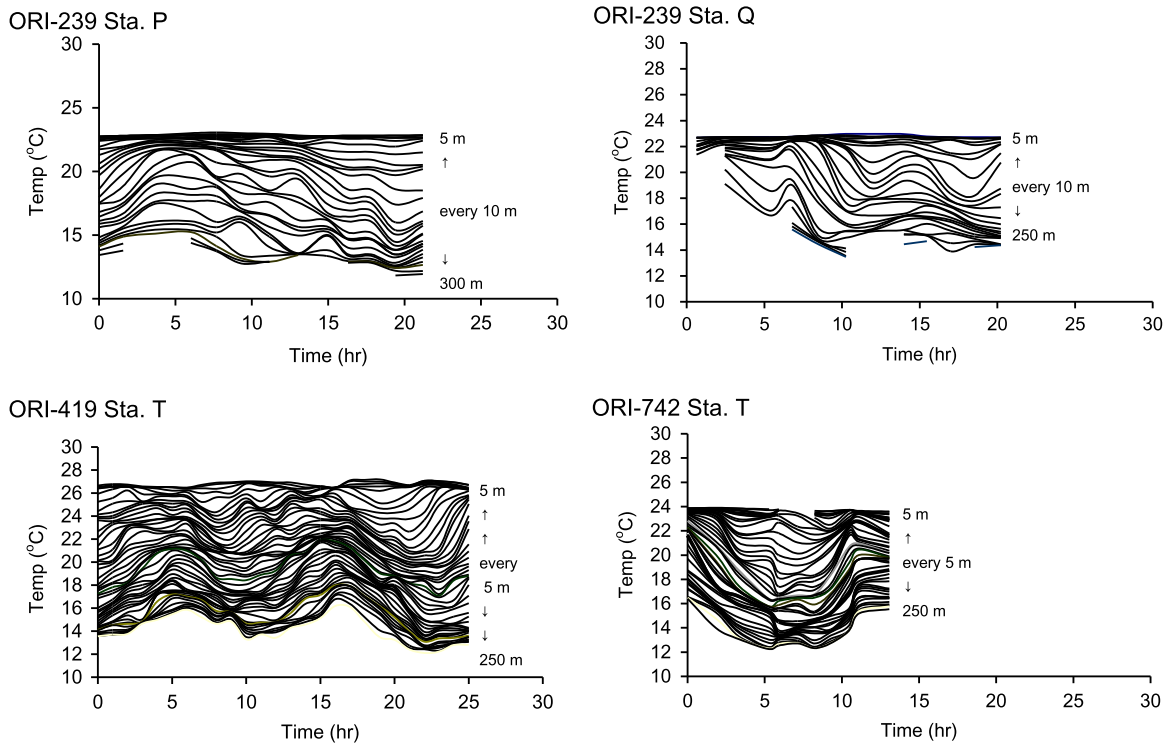

Fig. 3. Temporal variations of temperature at the fixed depths (from surface to bottom at 5 or 10 m intervals) for Cruise 239 at Stations P and Q, Cruises 419 and 742 at Station T.

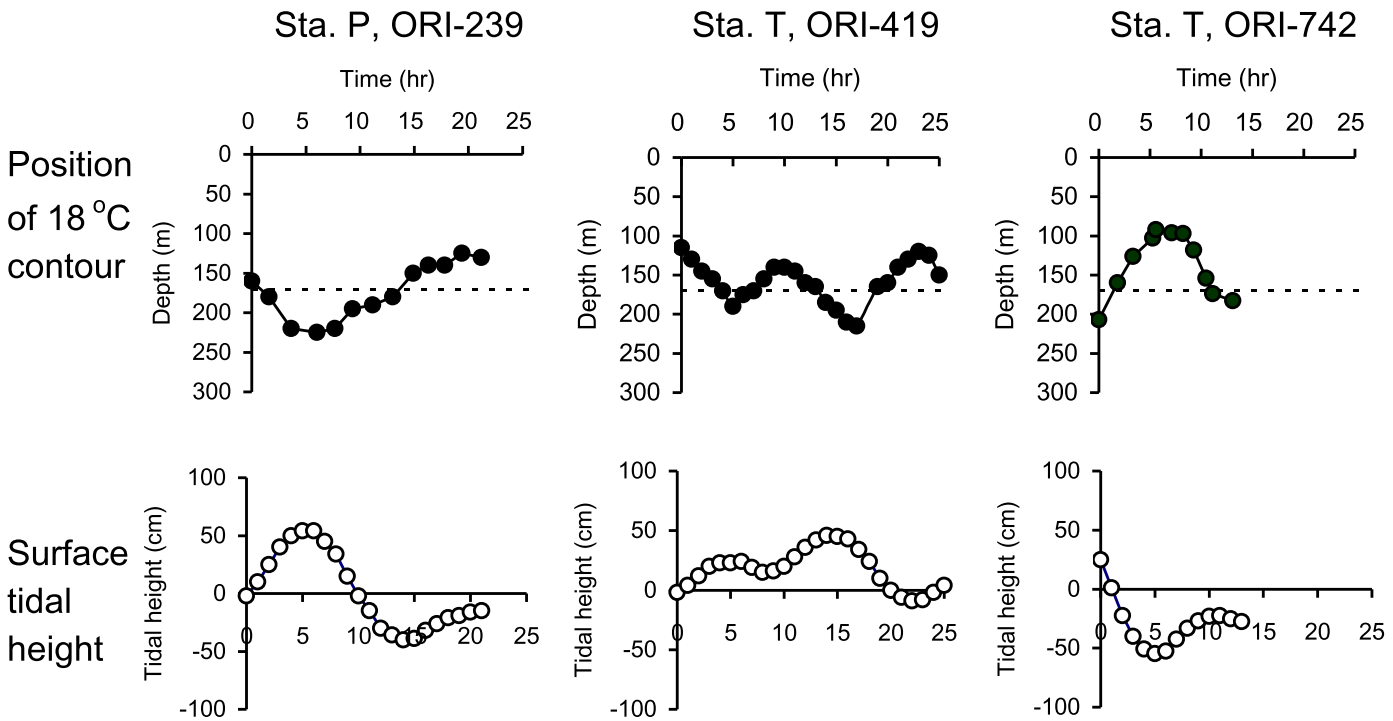

Fig. 4. (Up) Change of position of the 18 °C-isothermal line (m in depth) as observed on Cruises 239, 419 and 742. Dashed line marks the average oscillation center, i.e. 170 m. (Down) Surface tidal height (cm) recorded during the same periods at the Hsinguangdzu Tidal Station. It is obvious that the surface tide and the underwater movement are generally synchronized in frequency but almost opposite in phase.

tide due to the diffraction/refraction of Hengchun Peninsula, the arrival times may not be synchronized. The width and wavelength of the internal tide (Jan et al., 2008) are much larger than the length scale of both Hungtsai canyon and Hengchun Peninsula (ca. 100 *vs* 10 km), therefore the latter can hardly block the internal tidal movements. The consistent phase lag found here is rather complicated, but may be attributed to the orientation of the canyon and local topography.

3.4. Nutrient profiles

Oxygen and nutrient profiles obtained during Cruise 419 are

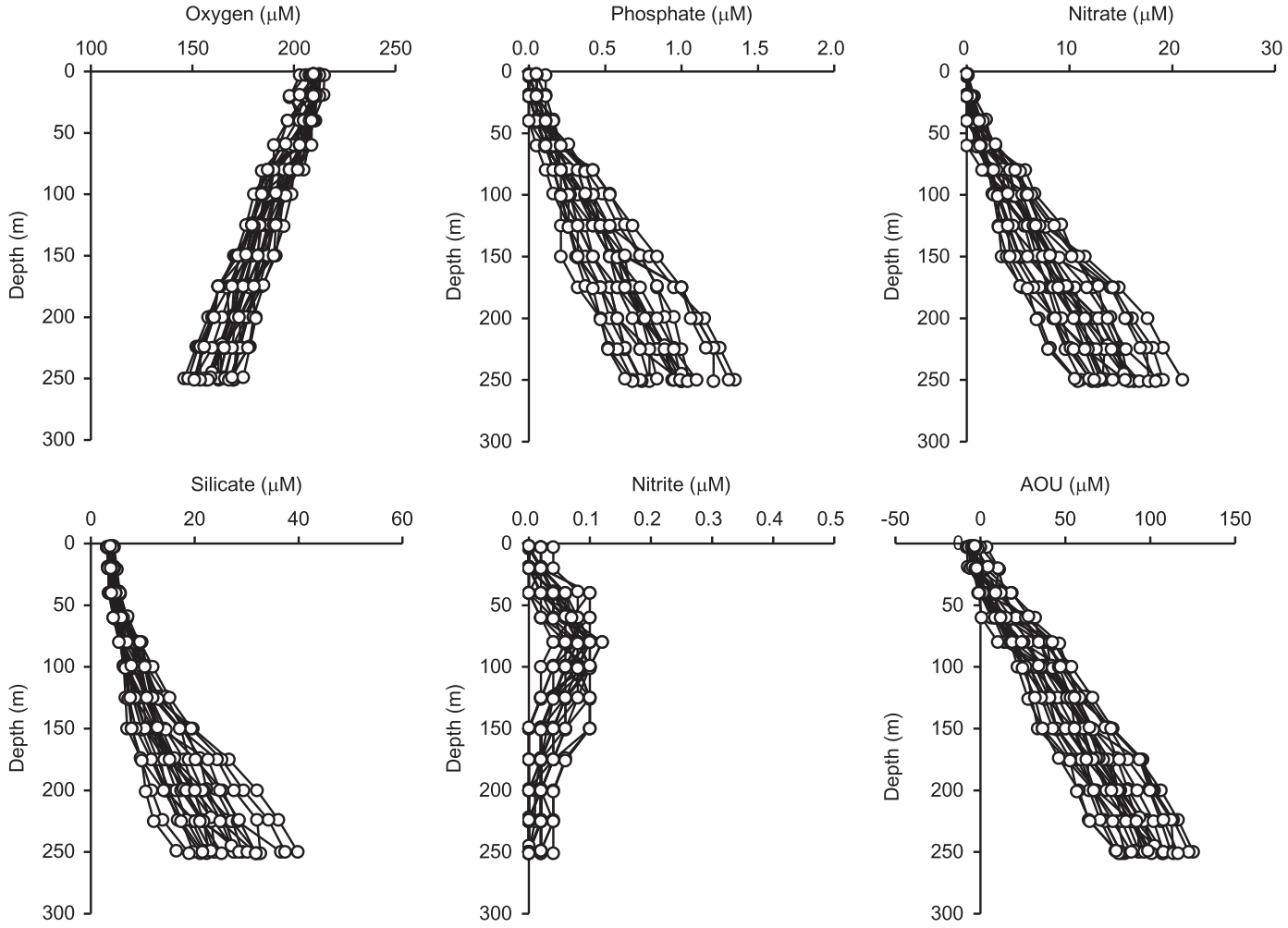

Fig. 5. Composite profiles (25 casts) of oxygen, nutrients and AOU at Sta. T on Cruise 419. The sampling frequency was ca. 1 cast per hr.

shown in Fig. 5. In general, the concentrations of nitrate, phosphate and silicate remain very low (almost depleted) in the upper 50 m layer, but increase with depth and vary with time. At the position of the trough rim at 100 m, the concentration ranges for nitrate, phosphate and silicates are 2-6 μM, 0.15–0.5 μM and 3–7 μM, respectively. At 175 m (near the 18 °C line), the corresponding concentration ranges are 5–14 μM, 0.3–0.9 and 7–21 μM, respectively. If the deeper water rises to higher than the trough rim at 100 m, the nutrient contents will mix promptly with the surface waters. When it sinks back into the trough, the nutrient concentrations in the downwelling water will be less than that of the upwelling water, thus resulting in a net upward nutrient flux.

3.5. Temporal variations

The data obtained from Cruise 419 were plotted against sampling time and shown in Fig. 6. All diagrams give a "W" pattern revealing two semidiurnal cycles of ca. 12 h periods. For every 6 h, the undersurface water layers (deeper than 70 m) moved either up or down, while the surface layers (0–50 m) were almost unaffected. The oscillation for all chemical items matched well with the physical parameters, which means that the short-term driving force, i.e. the internal tide, was overwhelming any biochemical process in this area.

An underwater salinity maximum layer of >34.6 which originates from the intrusion of the Kuroshio water was found between 18 and 21 °C. The water is also known as the South China Sea Tropical Water (Chen, 2005). The transmittance of this layer was low or the water was comparatively less clear. Just above this layer the water was with dense fluorescence, high in nitrite and oxygen. Below this layer the water became gradually rich in phosphate, nitrate and silicate, and the oxygen concentration became unsaturated. The 18 °C contour line is a good indicator to show this euphotic boundary.

3.6. Correlation plots

The relationships between different parameters provide further information relating to the mixing process of the water column. An end-member plot for each parameter against temperature has been carried out and the diagrams are shown in Fig. 7. From the T-S relationship diagram, it can be seen that the curve has two obvious turning points at 21 and 18 °C, respectively. The former (21 °C) refers to the rim of the trough at 100 m and the latter (18 °C) is the maximum oscillation.

The plots for nitrite and fluorescence are also given in Fig. 7. The maximum signals (nitrite 0.1 μM and fluorescence reading 0.8) are found at ca. 22.5 and 24.5 °C, respectively. The 18 °C line matches almost their bottom boundaries. The plots for nitrate, phosphate and silicate all show curvature relationships, but can be presented by three segmented broken lines with two major turning points at 15 °C and 18 °C. Each turning point can be treated as a relative end-member. The 15 °C can be related to a specific equal T-S layer where the two major water column types (the

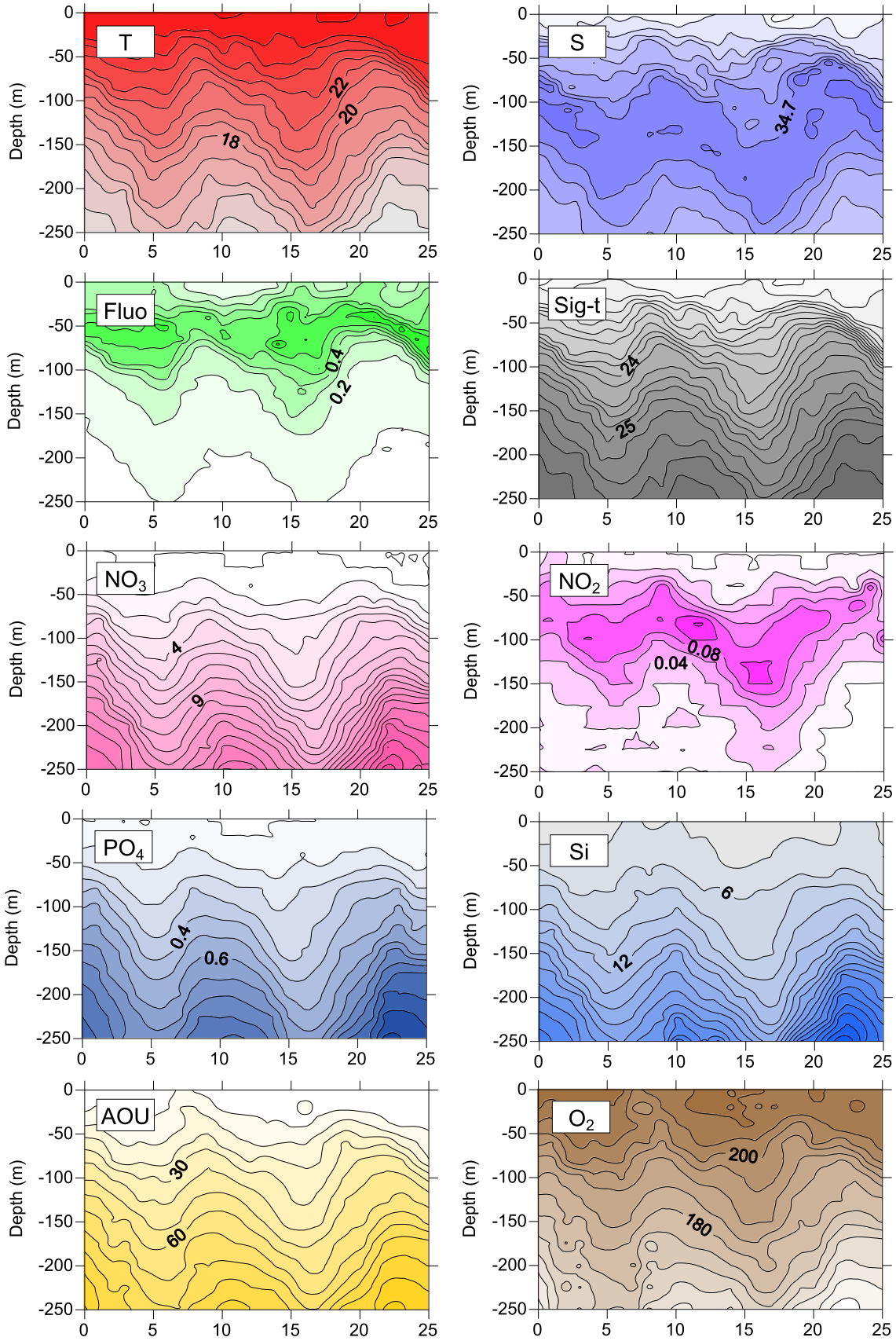

Fig. 6. Variation plots (over a 25-hr period) for data observed on Cruise 419. (Left column from top) temperature (°C), fluorescence, nitrate (μM), phosphate (μM) and AOU (μM); (right column from top) salinity, sigma-t, nitrite (μM), silicate (μM) and oxygen (μM).

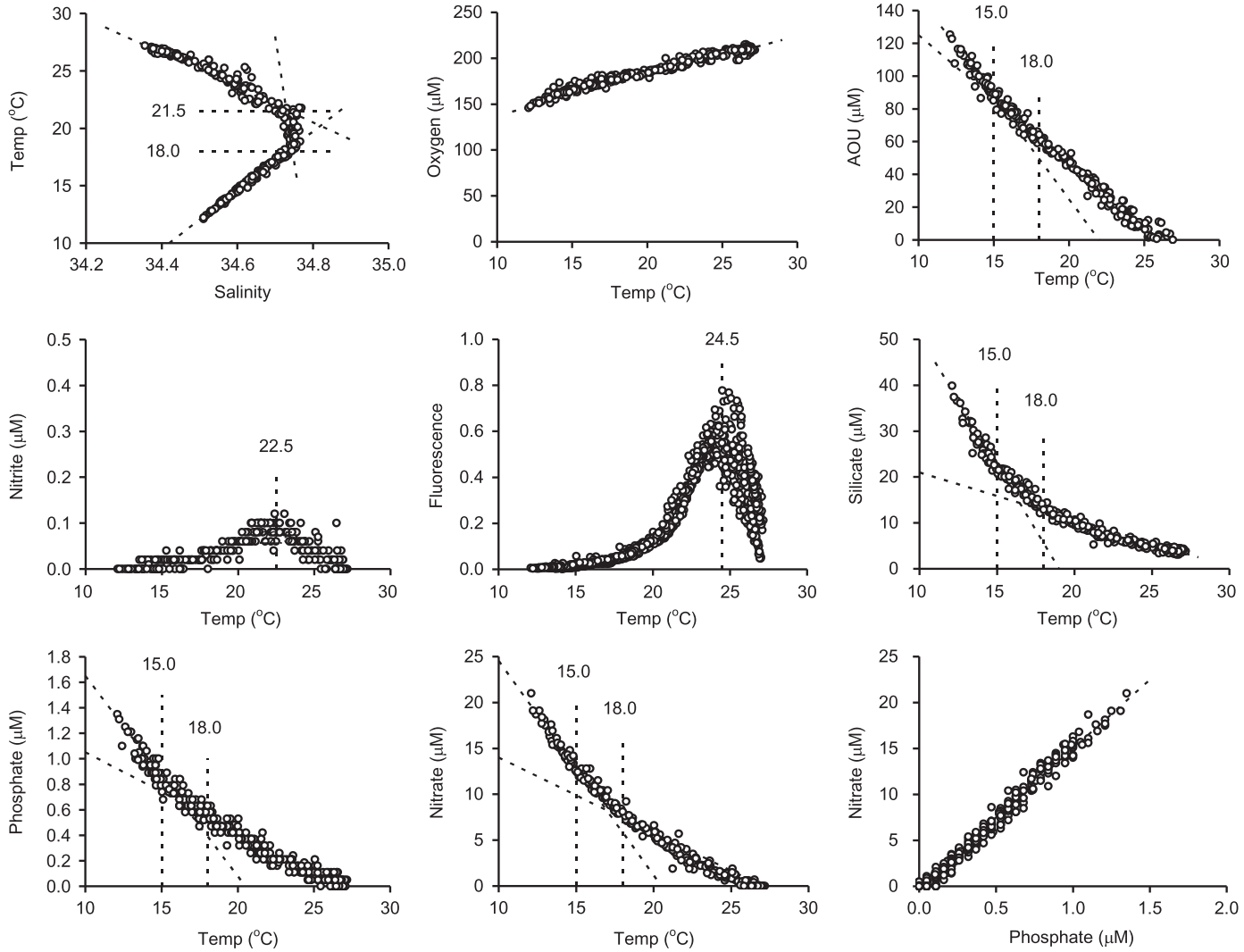

Fig. 7. Correlation plots against temperature for data taken from Cruise 419. Salinity, oxygen, AOU, nitrite, fluorescence, silicate, phosphate and nitrate were plotted against temperature. The nitrite and fluorescence maxima occurred at 22.5 and 24.5 °C, respectively. Each cross-over of auxiliary dashed lines (or the "turning point") can be treated as a relative end-member between water layers. The N/P ratio was estimated to be 14.8.

Philippine Sea type and the South China Sea type on a TS diagram) make a line-crossing at T=14.8 °C and S=34.57 (Pai et al., 2015). This point also refers to a boundary between the surface and intermediate layers (at ca. 250–300 m). At this point, the concentrations for the three nutrients are $[NO_3^-]$=15 μM, $[PO_4^{3-}]$=1.0 μM and [Si]=23 μM, respectively. This underlaying layer is mixed vertically with the water of the oscillation center. At 18 °C, $[NO_3^-]$=8.5 μM, $[PO_4^{3-}]$=0.6 μM and [Si]=15 μM.

When this water mass goes up and exposes above the trough edge, it is swept aside horizontally by the strong alongshore tidal current. The water is mixed with shelf water and the concentrations of nutrients are diluted. On the diagram the average concentrations at 21 °C are $[NO_3^-]$=4 μM, $[PO_4^{3-}]$=0.3 μM and [Si]=8 μM. When this water sinks into the trough during the surface spring tide, it mixes with the cold deep water to regain nutrients.

3.7. Nutrient fluxes

Jan and Chen (2009) have provided a simple method to evaluate the upward nutrient flux by multiplying the nutrient concentration by the average vertical moving speed. Accordingly, we treated the two turning points on the TS diagram (18 and 21 °C) as two nutrient source points representing the centers of the upwelling and downwelling movements. The average vertical speeds from Cruises 194, 239 and 742 was 19 m hr^{-1}. Thus, the upward fluxes for nitrate, phosphate and silicate are estimated to be 161.5 mmol N $m^{-2}hr^{-1}$, 11.4 mmol P $m^{-2}hr^{-1}$ and 285 mmol Si $m^{-2}hr^{-1}$. If this water is mixed with surface layer water, the temperature will be raised and the concentration of nutrients will be diluted. Using the nutrient data at 21 °C, the downward fluxes are 75 mmol N $m^{-2}hr^{-1}$, 5.7 mmol P $m^{-2}hr^{-1}$ and 152 mmol Si $m^{-2}hr^{-1}$. Although the upward and the downward fluxes may not be subtracted directly, it can still be concluded that the net values must be "upward-positive" and the scales of N and P fluxes are much larger than that reported for Nanwan Bay (Jan and Chen, 2009), revealing that tidal pumping in Hungtsai Trough can be a consistent nutrient supply.

A 3D diagram shown in Fig. 8, explains how the deep nutrient-rich water oscillates in the Hungtsai Trough and how the nutrients are carried away by the alongshore current. When the surface water flows in a southeast direction during the ebb tide, nutrient-rich bottom water will be raised up and some will be lifted above the shelf edge to mix with surface water. During the spring tide, the surface water flows in a northwest direction and the bottom water is drawn away from the trough, the surface low nutrient water sinks downwards to replenish the volume. Repeating the

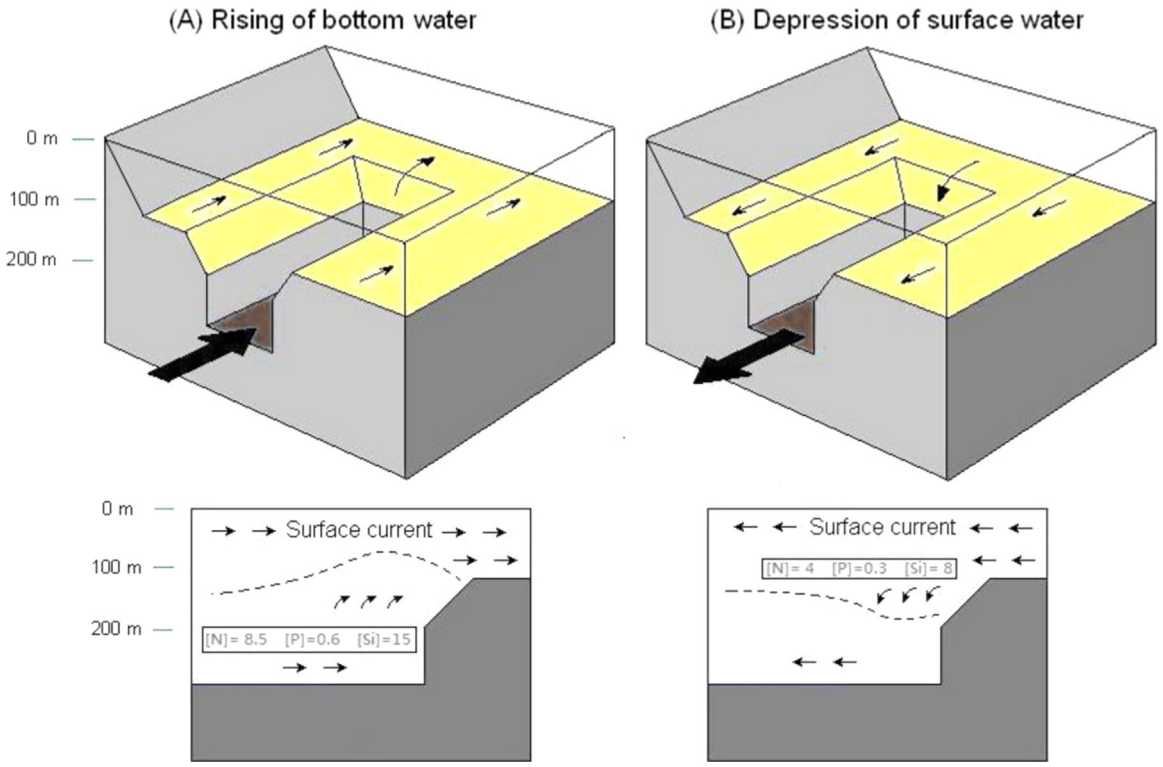

Fig. 8. Hypothetic 3D and transect diagrams demonstrating the vertical oscillation of nutrients in Hungtsai Trough. Dashed line denotes the upper boundary of the thermocline. (A) When the nutrient-rich deep cold water floods into the trough, some will be raised above the shelf edge and swept away by the surface current. (B) When the bottom water is drawn back from the trough, the surface water sinks downwards and replenishes the volume. The repeat process results in a net upward transportation of nutrients from bottom to surface. Numbers refer to the concentration of nutrients in μM units.

process results in a net upward transportation of nutrients from bottom to surface. Without the swept-aside mechanism the upwelled water may just sink back into the trough, so the net upward nutrient flux may not be as significant as what had been observed here.

4. Conclusion

Like Nanwan Bay and Kaoping Submarine Canyon, the Hungtsai Trough is another important nutrient upwelling source in southern Taiwan. Evidence has shown that the water column in Hungtsai Trough is subject to a very dynamic oscillation due to the strong internal tidal wave in the Luzon Channel. The largest daily temperature variation was found to be ca. 7 °C at 170 ± 10 m. It is convenient to draw an 18 °C contour line against time to show the vertical movement. The depth can be as shallow as 90 m and as deep as 240 m in a tidal cycle with an average amplitude of 110 m. The 18 °C line is also a bottom boundary for phytoplankton and nitrite, and the water mass refers to nutrient concentrations of 8.5, 0.6 and 15 μM for nitrate, phosphate and silicate, respectively. Thus, this nutrient-rich water acts as a nutrient end-member as indicated by the nutrient *vs* temperature plots. When it mixes with water above the shelf edge at 100 m, the nutrient concentrations are diluted to half of the values. The pumping up-then-sweeping aside process in this *cul-de-sac* (dead end) trough can be largely amplified; the positive net nutrients fluxes make the trough end like a point source of nutrients to the surface ecosystems. Similar processes have also been reported in many places, but the scales may not be as large as that observed here. A large proportion of the high productivity in the South China Sea can be attributed to this upwelling mechanism at many alongshore submarine canyons like the Hungtsai Trough.

Acknowledgment

The cruises were supported by the internship training program for master students of the Institute of Oceanography, National Taiwan University. The program was also sponsored partially by the National Science Council (now Ministry of Science and Technology), Taiwan. The authors would like to thank all participants, captain and crew of the RV Ocean Researcher I. The work is also dedicated to the memory of late Prof. K.K. Liu who initiated the first cruise. Suggestions by three anonymous reviewers are much appreciated.

References

Alford, M.H., Lien, R.C., Simmons, H., Klymak, J., Ramp, S., Yang, Y.J., Tand, D., Chang, M.H., 2010. Speed and evolution of nonlinear internal waves transiting the South China Sea. J. Phys. Oceanogr. 40, 1338–1355. http://dx.doi.org/10.1175/2010JPO4388.1.

Alford, M.H., MacKinnon, J.A., Nash, J.D., Simmons, H., Pickering, A., Klymak, J.Y., Pinkel, R., Sun, O., Rainville, L., Musgrace, R., Beitzel, T., Fu, K.H., Lu, C.W., 2011. Energy flux and dissipation in Luzon Strait: Two Tales of two ridges. Am. Meteological Soc. 41, 2211–2222. http://dx.doi.org/10.1175/JPO-D-11-073.1.

Alford, M.H., Peacock, T., MacKinnon, J.A., Nash, J.D., Buijsman, M.C., Centuroni, L.R., Chao, S.Y., Chang, M.H., Farmer, D.M., Fringer, O.B., Fu, K.H., Gallacher, P.C., Graber, H.C., Helfrich, K.R., Jachec, S.M., Jackson, C.R., Klymak, J.M., Ko, D.S., Jan, S., Johnston, T.M.S., Legg, S., Lee, I.H., Lien, R.C., Mercier, M.J., Moum, J.N., Musgrave, R., Park, J.H., Pickering, A.I., Pinkel, R., Rainville, L., Ramp, S.R., Rudnick, D.L., Sarkar, S., Scotti, A., Simmons St, H.L., Laurent, L.C., Venayagamoorthy, S.K., Wang, Y.H., Wang, J., Yang, Y.J., Paluszkiewicz, T., Tang, T.Y., 2015. The formation and fate of internal waves in the South China Sea. Nature 521, 65–69. http://dx.doi.org/10.1038/nature14399.

Bosley, K.L., Lavelle, J.W., Brodeur, R.D., Wakefield, W.W., Emmett, R.L., Baker, E.T., Rehmke, K.M., 2004. Biological and physical processes in and around Astoria submarine Canyon, Oregon, USA. J. Mar. Syst. 50, 21–37. http://dx.doi.org/10.1016/j.jmarsys.2003.06.006.

Chen, C.C., Shiah, F.K., Lee, H.J., Li, K.Y., Meng, P.J., Kao, S.J., Tseng, Y.F., Chung, C.L., 2005. Phytoplankton and bacterioplankton biomass, production and turnover

in a semi-enclosed embayment with spring tide induced upwelling. Mar. Ecol. Prog. Ser. 304, 91–100.
Chen, C.T.A., Wang, B.J., Hsing, L.Y., 2004. Upwelling and degree of nutrient consumption in Nanwan Bay, Southern Taiwan. J. Mar. Sci. Technol. 12 (5), 442–447.
Chen, C.T.A., 2005. Tracing tropical and intermediate waters from the South China Sea to the Okinawa Trough and beyond. J. Geophys. Res. 110, C05012. http://dx.doi.org/10.1029/2004JC002494.
Chiou, M.D., Jan, S., Wang, J., Lien, R.C., Chien, H., 2011. Sources of baroclinic tidal energy in the Gaoping Submarine Canyon off southwestern Taiwan. J. Geophys. Res. 116, C12016. http://dx.doi.org/10.1029/2011JC007366.
Farmer, D., Li, Q., Park, J.H., 2010. Internal wave observations in the South China Sea: the role of rotation and nonlinearity. Atmosphere-Ocean 47, 267–280. http://dx.doi.org/10.3137/OC313.2009.
Jan, S., Chern, C.S., Wang, J., Chao, S.Y., 2007. Generation of diurnal K-1 internal tide in the Luzon Strait and its influence on surface tide in the South China Sea. J. Geophys. Res. -Ocean. 112 (C6), C06019-C06019.
Jan, S., Chen, C.T.A., 2009. Potential biogeochemical effects from vigorous internal tides generated in Luzon Strait: a case study at the southernmost coast of Taiwan. J. Geophys. Res. 114, C04021. http://dx.doi.org/10.1029/2008JC004887.
Jan, S., Lien, R., Ting, C., 2008. Numerical study of baroclinic tides in Luzon Strait. J. Oceanogr. 64, 789–802.
Ko, D.S., Chao, S.Y., Huang, P., Lin, S.F., 2009. Anomalous upwelling in Nan Wan July 2008. Terr. Atmos. Ocean. Sci. 20 (6), 839–852. http://dx.doi.org/10.3319/TAO.2008.ll.25.0l(Oc).
Lee, H.J., Chao, Y., Fan, K.L., Wang, Y.H., Liang, N.K., 1997. Tidally induced upwelling in a semi-enclosed basin: Nan Wan Bay. J. Oceanogr. 53, 467–480.
Lee, I.H., Wong, Y.H., Liu, J.T., Chung, W.S., Xu, J., 2009. Internal tidal currents in the Gaoping (Kaoping) Submarine Canyon. J. Mar. Syst. 76, 397–404. http://dx.doi.org/10.1016/j.jmarsys.2007.12.011.
Liang, N.K., Chang, J.G., Su, C.H., Wang, K.I., 1985. Data report of temperature and current measurement in the Hung-Tsai Trough off southern Taiwan, Special Report #19. Institute of Harbor and Marine Technology, Taiwan, p. 122.
Liang, W.D., Tang, T.Y., Yang, Y.J., Ku, M.T., Chuang, W.S., 2003. Upper-ocean currents around Taiwan. Deep Sea Res. II 50, 1085–1105. http://dx.doi.org/10.1016/S0967-0645(03)00011-0.
Lien, R.C., Tang, T.Y., Chang, M.H., Asaro, E.A.D., 2005. Energy of nonlinear internal waves in the South China Sea. Geophys. Res. Lett. 32, L05615. http://dx.doi.org/10.1029/2004GL02212.
Lien, R.C., Henyey, F., Ma, B., Yang, Y.J., 2014. Large-amplitude internal solitary waves observed in the northern South China Sea: properties and energetics. J. Phys. Oceanogr. 44, 1095–1115. http://dx.doi.org/10.1175/JPO-D-13-088.1.
Pai, S.C., Jan, S., Chu, K.S., Huang, P.Y., Takahashi, M.M., 2015. Kuroshio or Oyashio - Sources of the 700 m deep ocean water off Hualien coast, eastern Taiwan. Deep Ocean Water Res. 15 (3), 107–116.
Rennie, S.J., Pattiaratchi, C.B., McCauley, R.D., 2009. Numerical simulation of the circulation within the Perth Submarine Canyon, western Australia. Cont. Shelf Res. 29, 2020–2036.
Shea, R.E., Broenkow, W.W., 1982. The role of internal tides in the nutrient enrichment of Monterey Bay, California. Estuar. Coast. Shelf Sci. 15, 57–66.
Yu, H.S., Chiang, C.S., 1994. Morphology and origin of the Hongtsai submarine canyon west of the Hengchun Peninsula, Taiwan. J. Geol. Soc. China 38 (1), 81–92.
Wei, C.L., Chou, L.H., Tsai, J.R., Wen, L.S., Pai, S.C., 2009. Comparative geochemistry of ^{234}Th, ^{210}Pb, and ^{210}Po: A case study in the Hung-Tsai Trough off southwestern Taiwan. Terr. Atmos. Ocean. Sci. 20 (2), 411–423. http://dx.doi.org/10.3319/TAO.2008.01.09.01(Oc).
Wei, C.L., Jiann, K.T., Wen, L.S., Sheu, D.D.D., 2012. Distributions and removal fluxes of trace metals in the water column of the Hung-Tsai Trough off southwestern Taiwan. Mar. Pollution Bull. 64, 1122–1128. http://dx.doi.org/10.1016/j.marpolbul.2012.03.032.